Refereed Proceedings

The 12th International Conference on Fluidization - New Horizons in Fluidization Engineering

Engineering Conferences International *Year* 2007

Scale-Up Effect on Heat Transfer in a Fluidized Bed Near the Onset of Turbulent Fluidization

A. Stefanova* John R. Grace† C. Jim Lim‡

Xiaotao T. Bi** K.S. Lim†† J. Sanderson‡‡

*University of British Columbia, astefano@chml.ubc.ca

†University of British Columbia, jgrace@chml.ubc.ca

‡University of British Columbia, cjlim@chml.ubc.ca

**University of British Columbia, xbi@chml.ubc.ca

††CSIRO Minerals, Seng.Lim@csiro.au

‡‡CSIRO Minerals, John.Sanderson@csiro.au

SCALE-UP EFFECT ON HEAT TRANSFER IN FLUIDIZED BEDS NEAR THE ONSET OF TURBULENT FLUIDIZATION

A. Stefanova[1], J. R. Grace[1], C. J. Lim[1], H.T. Bi[1], K.S. Lim[2], J. Sanderson[2],
[1] University of British Columbia, Department of Chemical and Biological Engineering,
2360 East Mall, Vancouver, Canada V6T 1Z3.
[2] CSIRO Minerals, Box 312, Clayton VIC 3169 Australia.

ABSTRACT

Heat transfer coefficients were measured in 0.29 m ID and 1.56 m ID fluidization columns with the same heater tube, identical alumina particles and geometrically scaled distributors. The maximum coefficients occurred in the turbulent fluidization flow regime. The Froude number based on superficial velocity and column diameter captures the scale-up effect well, so long as the heater is located in a region of similar flow structure.

INTRODUCTION

High heat transfer coefficients and uniform temperatures are major reasons why fluidized beds are widely used in many commercial applications such as chemical production, drying, coating, roasting. Research on heat transfer in fluidized beds has been carried out for several decades, and the mechanism of heat transfer is generally well established for bubbling and fast fluidized beds. However, little work has been done to understand the mechanism of heat transfer in the transition region between bubbling and fast fluidization, known as turbulent fluidization. Many commercial units using Geldart group A or AB particles and superficial gas velocities from 0.3-0.8 m/s are operating in this flow regime.

There are three components of heat transfer: convection by particles, convection by gas and radiation. For temperatures <600°C and small particles, the particle convection component is the most significant. The particle convection heat transfer was found to depend on frequency of particles exchange at the heater surface and particle concentration near the heater surface (Mickley & Fairbanks 1955). A maximum heat transfer coefficient, h_{max}, (although usually not very pronounced and occurring over a range of velocities) has been observed in many studies with increasing gas velocity. It occurs because decreasing particle concentration ultimately counterbalances the increasing frequency of particle exchange. Zabrodsky (1966) established a correlation for the superficial velocity, U_{opt}, at which h_{max} occurs for group B particles and laboratory scale columns. Some studies (Sun & Chen 1989, Basu & Dieh 1985, Staub, 1979) suggest that the maximum heat transfer coefficient coincides with the superficial velocity, U_c, at the onset of turbulent fluidization. Among published correlations, U_{opt} is usually lower then U_c. The relationship between U_{opt} and U_c is currently unclear. In addition, uncertainty related to determining U_c, arising from different experimental methods and transition criteria (Brereton and Grace, 1991; Bi and Grace, 1995; Rhodes, 1996) adds to the challenge.

To be able to apply laboratory scale data to large commercial units, knowledge of the effect of scale–up on bed hydrodynamics is required. Larger units have been reported to give higher mixing rates and to exhibit different flow structures than scaled-down counterparts (Matsen 1996). Increased diameter and lower H/D_t have been found to decrease the transition velocity U_c (Sun & Chen 1989, Ellis et al. 2004). It is important to investigate how heat transfer is affected by changes in hydrodynamics and reactor scale,

The 12th International Conference on Fluidization - New Horizons in Fluidization Engineering, Art. 32 [2007]

as well as the relationship between flow regime transition and maximum heat transfer. The objective of this work is to examine the effect of the transition to turbulent fluidization on the bed-to-surface heat transfer in columns of different diameter.

EXPERIMENTAL METHODS

Two fluidization columns were used in the experiments. The smaller, Plexiglas column, 0.29 m ID and 4.5 m high, is located at the University of British Columbia, Canada, whereas the larger one, steel, 1.56 m ID and 12 m high, resides at CSIRO Minerals, Clayton, Australia. Both are described in Ellis et al. (2004). Air was supplied by Roots blower, measured by an orifice plate and distributed by 18 bubble caps in both columns. The distributors were geometrically similar, giving open area ratio of 0.9%. More details on the bubble cap distributors are given by Sanderson and Rhodes (2003). The solids return system of the smaller column consisted of two cyclones at the top of the column and two return legs and was controlled by a pressure balance across a flapper valve. The large column was equipped with two cyclones near its top. Particles captured by the cyclones returned to the bed through an aerated loop seal. To achieve better collection efficiency only one side of the solids return system was used. With the entrance to the other side of the solids return system sealed. The solids not captured by the cyclone entered the exhaust line and were collected in a bag filter.

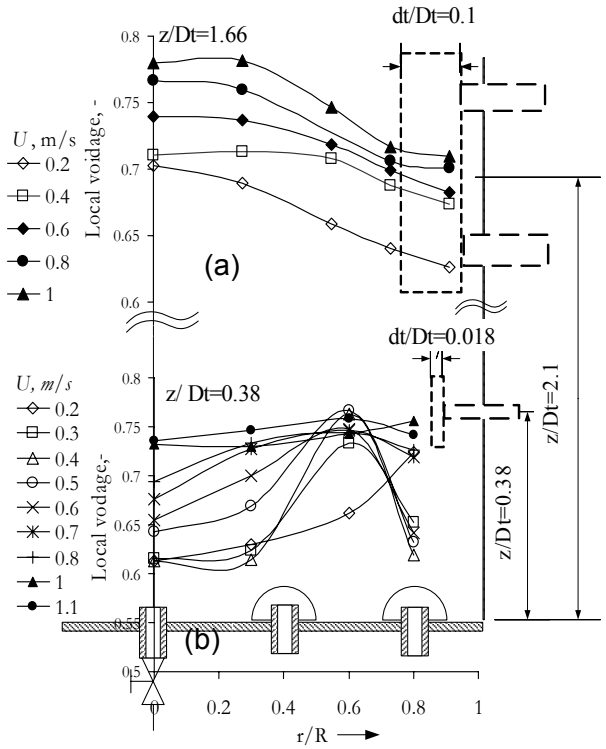

Figure 1. Radial distribution of local voidage: a) D_t=0.29 m, z=0.475 m; b) D_t=1.56 m, z=0.6 m.

Heat transfer coefficients were determined using an electrically heated copper tube 28.6 mm OD and 101 mm long. Hemi-spherical teflon pieces at the tube ends minimized heat losses and flow disturbances. Four T-type thermocouples were installed, two attached to the copper surface, and two near the tube ends for heat loss estimation. In the 0.29 m column the heater tube was positioned at different radial locations by two horizontal tubes, whereas in the 1.56 m column it was installed on a traversing arm (38.1 mm OD), together with the optical probe. In both columns the heater was 0.6 m above the distributor. Power to the heater was supplied by a DC power source, Tenma 72-7295, with adjustable voltage. The heat transfer coefficient, h was calculated from:

$$h = \frac{VI - Q_l}{A_s (T_s - T_b)} \qquad (1)$$

The voltage V and current I supplied to the heater were logged to the data acquisition system using a voltage divider and current sensor. Heat losses, Q_l were estimated to be in the range 2-4% of the total power supplied to the heater for heat transfer coefficients of 100-400 W/m^{2}K. Bed temperature T_b was measured by T-type thermocouples. The uncertainty of the measured heat transfer coefficient within 95% confidence level, including the heat losses, was estimated to be 5% (Coleman & Steele, 1998).

The hydrodynamics of the bed were evaluated using optical probes and Omega 142PC series differential and absolute pressure sensors, connected to pressure taps flush with the column wall. Bed expansion, mean bed voidage and cross-sectional mean bed voidage were obtained from time-mean pressure measurements. Local voidages in the 0.29 m ID column were measured by optical probes above and below the heater, 0.75 m and 0.48 m above the distributor plate, respectively. In the 1.56 m column, there was only one optical probe 0.6 m above the distributor plate. The optical probes and heaters were traversed radially in both columns.

Data were logged via 32-channel expansion boards and Computer Boards DAS08 analog/digital converter to a PC. Once steady state had been reached, the heat transfer data were recorded for a 5-10 minutes period with a 5 s sampling time using a custom-made Visual Basic program. Pressure and local voidage fluctuations were recorded for periods of 100 s at a sampling frequency of 50 Hz using Labtech Notebook software. The particles in both columns were calcined alumina particles from the same batch with mean diameter 80 μm and density 2700 kg/m^3. The loose packed bed voidage was ε_0=0.6, and U_{mf}=0.007 m/s. The static bed height was 0.8 m in both columns.

RESULTS AND DISCUSSION

Circulation patterns and local voidage distribution

Two important hydrodynamic features for the particle convection component of heat transfer are the particle concentration and the frequency of exchange of particles at the heater surface. Both are affected by the circulation patterns in the bed. Due to the different H_0/D_t ratios in the two columns it was expected that the circulation patterns in the bed would differ. The radial profile of the local voidage is given in Figure 1. The highest voidage was measured in the central region of the smaller column, whereas in the larger column, the highest voidage was found at r/R=0.6. The smaller column also exhibited more uniform profiles than the larger one at low gas velocities.

In the larger column, because the bed is relatively shallow (H_0/D_t=0.6), the distributor significantly affects the flow and circulation patterns. Voids formed at the distributor do not fully coalesce before reaching the top of the bed. The circulation pattern was typical of shallow beds, with voids rising primarily near r/R=0.5 and downwards bulk solids movement at the centre of the column and near the outer wall (leading to “gulf streaming”). At low gas velocities, U≤0.2 m/s, most voids rose closer to the wall (r/R=0.8), probably attributable to uneven distribution of gas by the bubble cap distributor. Note that the central bubble cap was blocked off in both columns. In the smaller column the bed was deep enough for voids formed at the distributor to fully coalesce and rise in the centre of the column. Particles are carried up by the voids in the central region of the column, and descend near the wall.

Pressure fluctuations and onset of turbulent fluidization

With increasing superficial gas velocity, the standard deviations of pressure fluctuations, σ_{AP}, increased in the 0.29 m ID column, reached a maximum between 0.6 and 1 m/s and then decreased slightly (Figure 2). No significant effect of the radial location of the immersed heater tube was observed. The standard deviation of pressure fluctuations in the large column was nearly constant from 0.2 to 0.4 m/s, started to increase beyond 0.4 m/s, and reached a maximum for $U \approx 1$ m/s.

Normalizing σ_{AP} by dividing by the time mean pressure shifts the maximum to lower velocities: U_{cN}=0.4 m/s for D_t=0.29 m/s, and U_{cN}=0.98 m/s for D_t=1.56 m (Bi & Grace, 1995). Normalised σ_{AP} is plotted against the Froude number, $Fr=U/(gD_t)^{0.5}$, (Glicksman et al.,1993) in Figure 3. The maxima estimated from third order polynomials, least square fitted through the data points, occur at similar Fr for the two columns.

Features specific to turbulent fluidization like break-up of large voids, increased

The 12th International Conference on Fluidization - New Horizons in Fluidization Engineering, Art. 32 [2007]

homogeneity of the bed, increased particle entrainment and change in local voidage trends (Figure 4) are observed in the range 0.4-0.6 m/s for the 0.29 m ID column and 0.8-1 m/s for the 1.56 m ID column. This indicates that the onset of turbulent fluidization occurred at lower U in the smaller column, contrary to findings reported by Sun & Chen (1989) and Ellis et al. (2004). Note, however, that their studies were performed without immersed objects, with different distributors, and with smaller and lighter catalyst particles. Staub (1979) reported that immersed tube banks shift the transition to the turbulent fluidization flow regime to lower superficial gas velocities. Considering that the heater was not geometrically scaled and the ratio d_t/D_t is 0.1 for the smaller column, but only 0.018 for the larger column, the heater is expected to affect the local flow more in the smaller column. Such an effect could not, however, be detected by pressure fluctuations at the column wall in the smaller column (Figure 2).

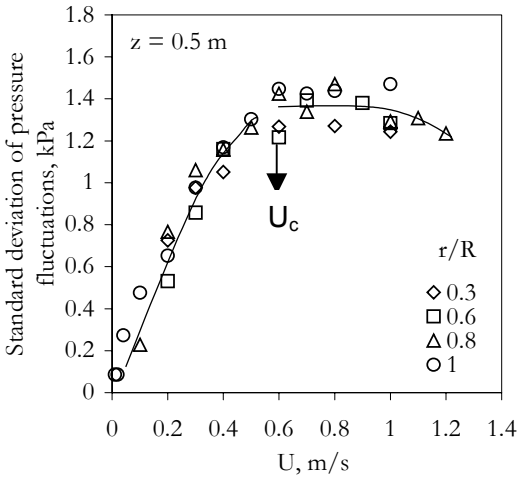

Figure 2. Standard deviation of pressure fluctuations, D_t=0.29 m

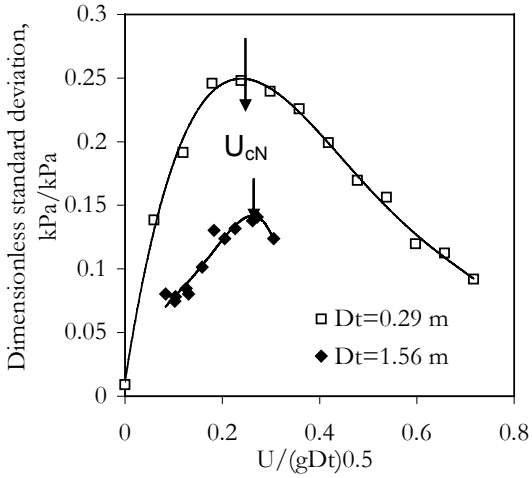

Figure 3. Dimensionless standard deviation of pressure fluctuations

Heat transfer and local flow structure transition

Particles in the bed can travel as a part of emulsion, bubble wakes or clusters (Mostoufi & Chaouki, 2004). Any change in the mechanism of transport of particles with increasing gas velocity is likely to affect the particle contact at the heater surface, and thus the heat transfer. The effect of increasing superficial gas velocity on the measured heat transfer coefficients and local voidage at different radial positions is plotted for both columns in Figure 4:

0.29 ID Column

In the smaller column, h increased steeply with increasing U after the onset of bubbling. As the gas velocity increased, larger faster bubbles formed and the frequency of exchange of particles at the heat transfer surface increased, augmenting the heat transfer coefficient. The trend changes noticeably in the range $0.2<U<0.6$ m/s, depending on the radial location of the heater. The optimum velocity for heat transfer, U_{opt}=0.17 m/s, calculated from Todes' correlation (Zabrodsky, 1966) is close to that observed for r/R=0. Near U=0.2 m/s, the mean bubble size is $D_b \approx 0.5 D_t$ (Mori & Wen, 1975) and the bubble size, velocity and frequency are all significantly influenced by wall effects (Hovmand & Davidson, 1971). This affects the frequency of particle exchange at the heater surface and hence the heat transfer coefficient. Although the criteria for onset of slugging were satisfied ($U_{Dbmax}>U>U_{ms}$=0.12 m/s and $z_{sl}<H$), typical slugging

was never observed. Individual voids passing along the heater were identified by cross-correlating the signal from two vertically aligned optical probes fixed above and below the heater, 0.275 m apart. The cross-correlation function shows a strong positive peak at a time lag of ~0.2 s for U=0.2 m/s and r/R=0. As the gas velocity increased, the peak became less pronounced, and beyond 0.4 m/s the estimated cross-correlation coefficients were widely distributed among time lags. The presence of the immersed heater in the column and its horizontal support tubes, in addition to a significant proportion of fines in the bed, might account for instability of large voids, causing them to split at the bottom of the heater. Nevertheless, periodic fluctuations associated with slugging were observed intermittently, interspersed with periods of more random fluctuations typical of a turbulent flow structure up to 1 m/s. The heat transfer coefficient profiles follow the trend of the local voidage at the corresponding radial position in the range 0.1≤U<0.5 m/s, indicating that the dominant influence of the void patterns and frequencies on solids renewal at the heater surface.

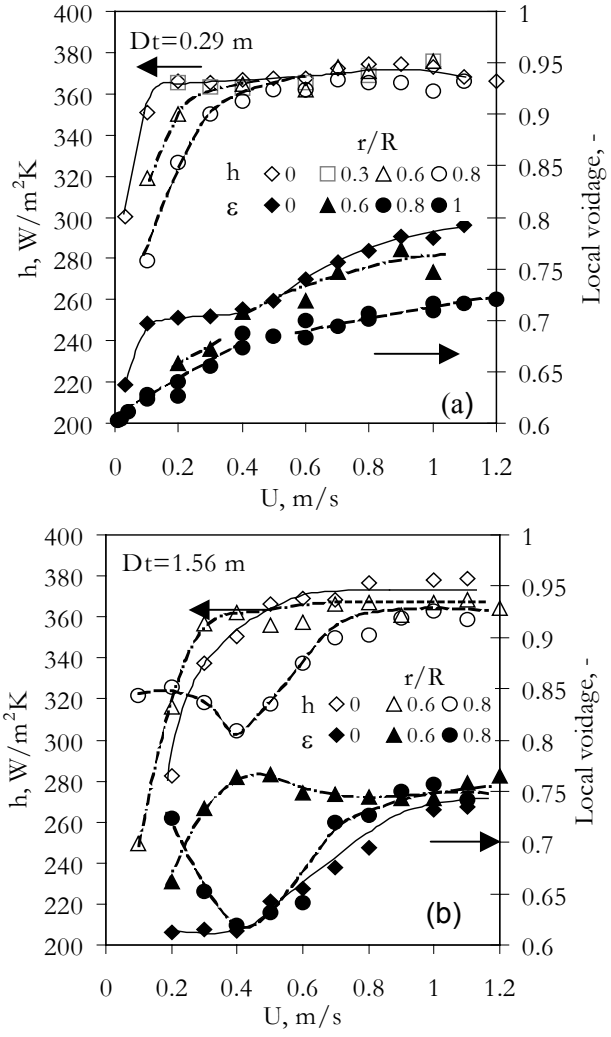

Figure 4.Variation of time-mean heat transfer coefficient and local voidage for the two columns.

The difference between h at the centre and near the wall slowly diminished as the gas velocity increased, with the heat transfer coefficient becoming independent of U and r/R beyond U ≈0.6 m/s. These trends can be attributed to changes in local flow structure. From the plot of the local voidage in Figure 4(a), it is evident that there is a change in trend of the local voidage in the superficial velocity range of 0.4 to 0.6 m/s. Macroscopic changes such as increased entrainment of particles and maximum pressure fluctuations (Figure 2) are observed close to 0.6 m/s. It is likely that the onset of turbulent fluidization takes place at U = 0.4-0.6 m/s. The flow structure in turbulent fluidization is characterized by a gradual breakdown of the bubble/emulsion phase, replaced by short-lived unstable voids of irregular shape, containing significant amounts of particles and particle clusters. With this evolution of the flow structure, bubbles are no longer the “driving force” for particle circulation in the bed.

The increasing local voidage has negligible effect on h for 0.6≤U<1 m/s. Hamidipour et al. (2005b) measured contact frequencies of particles and found a wider distribution in the turbulent regime than for bubbling/slugging. Hamidipour et al. (2005a) also reported that for sand (B group) particles, the particle contact time decreased with increasing U, reaching a

The 12th International Conference on Fluidization - New Horizons in Fluidization Engineering, Art. 32 [2007]

minimum at the onset of turbulent fluidization and then increasing. For FCC (group A) particles, U did not have a significant effect on the particle contact time. Our alumina particles fall near the AB boundary in Geldart's classification, and it is uncertain which trend they will follow. However, two mechanisms are possible: (a) The frequency of exchange of particles increases in the turbulent fluidization flow regime, but its effect is balanced by the increased voidage. (b) The frequency of exchange of particles is unaffected by U in turbulent fluidization region, and the increased voidage has an insignificant effect on the heat transfer. The frequency of particle contact with the heater surface at low gas velocities can be estimated from the frequency of bubbles (Mckain et al. 1994). For U=0.2 m/s and r/R=0, the dominant frequency of the optical probe signal occurred at ~1.3 Hz and decreased to 0.6 Hz with increasing U. The latter is similar to the particle contact frequencies reported by Hamidipour et al. (2005b). In the turbulent fluidization regime, the dominant frequency from the optical probe signal could not be unambiguously identified. Further analysis of the optical probe signal, e.g. use of cycle frequency, might yield more information.

1.56 m ID Column

In the 1.56 m ID column the heat transfer coefficients follow trends similar to those in the smaller column, except at r/R=0.8, i.e. in the wall region. Maximum h is first reached for r/R = 0.6 and $U \approx 0.4$ m/s. This velocity is greater than U_{opt}, but closer to the velocity at which bubbles reach their maximum size. At low gas velocities, heat transfer in this region of the bed is promoted by frequent particle exchange due to bubbles passing the heat-transfer surface.

In the central region of the column, i.e. r/R = 0 and 0.3, h_{max} is reached more gradually. Although the local voidage is close to that at minimum fluidization conditions for U≤0.4 m/s, h has comparable values and follows the same trend as at r/R=0.6. It might be expected that, due to the absence of voids in the central region, particle exchange at the surface would decrease (similar to the wall region for the smaller column), resulting in lower h, but this was not the case. It appears that this region is strongly influenced by the rising voids at r/R=0.6. Bulk particle motion ("gulf streaming") with velocities comparable to those of the rising voids might be responsible for bringing fresh particles to the heater surface in the central region. Alternatively, the higher particle concentration could lead to more particles contacting the surface, compensating for the lower renewal frequency.

Near the wall, at r/R=0.8, the heat transfer coefficients were affected more by the change in local voidage than in the central region. At low gas velocities (U~0.2 m/s), the presence of the voids near the wall promotes exchange of particles at the heater surface, leading to higher heat transfer coefficients. Individual voids were detected from the optical probe and differential pressure signals, with dominant frequency ~1.8 Hz. As the vertical trajectory of voids gradually approaches r/R=0.6, h starts to decrease in the wall region, reaching a minimum close to 0.4 m/s. Although the heater was in a region of high particle concentration for 0.3≤U≤0.5 m/s, the particle exchange was limited due to the wall effect on the bulk movement of particles. This suggests that the frequency of renewal of particles at the surface is more influential than the particle concentration. For U beyond 0.4 m/s, the local flow structure changes, as more gas enters the dense phase in the central region and towards the walls, gradually creating a more homogenous flow structure across the bed. Once this transition was complete (U>0.9 m/s), radial profiles of local voidage became flat (Figure 1), and h at different radial locations had similar values, and did not vary significantly up to the highest U investigated. At gas velocities high enough to expose the heater due to major entrainment, it is expected that h will begin to decrease.

The measured heat transfer coefficients in the two columns are plotted against $Fr = U/(gD)^{0.5}$ in Figure 5. Where the flow structures near the heater are similar, the heat

transfer coefficients are similar for the same values of Fr. At lower Fr (e.g. for $Fr \lesssim 0.1$ in the core of the column where there is a high presence of bubbles or for $Fr \lesssim 0.26$ near the wall) the curves diverge. For the experimental points at r/R=0.8 and low U (Fr < 0.1) in the larger column (Figure 5, filled circles) the mechanism controlling the heat transfer is similar to that in the central region of the smaller column. Consequently, the data points are closer to the r/R=0 curve (open diamonds) of the smaller column. For Fr<0.26 and the region of the bed not characterized by high bubble concentration nor near the column wall, the heat transfer coefficients fall between those corresponding to r/R=0 and r/R=0.8. It appears that beyond Fr=0.26, h becomes independent of r/R for both columns. This critical Fr corresponds to the maximum normalized standard deviation of absolute pressure fluctuations at the column wall for both columns.

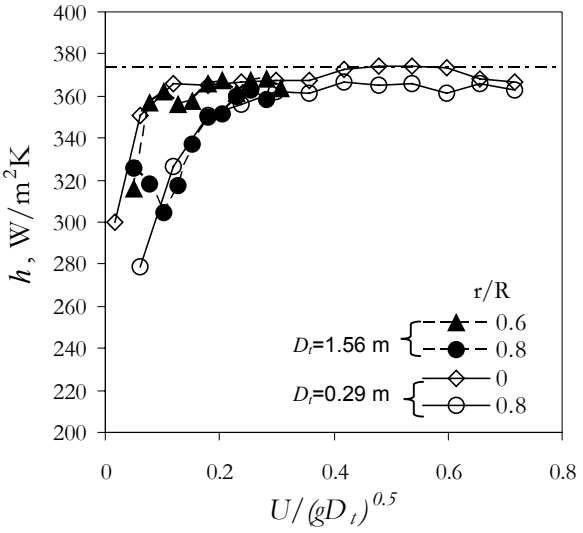

Figure 5. Heat transfer coefficient at different radial locations vs. Froude number.

CONCLUSION

The superficial gas velocity at which the bed-to-surface heat transfer coefficient changes its trend and reaches a maximum was found to increase with increasing column diameter and was affected by the radial location of the heater for the experimental conditions of this study. The heat transfer coefficient followed a different trend at lower gas velocities in regions of higher voidage (high bubble presence) compared to the region near the wall in both columns. Since the frequency of exchange of particles at the surface is affected by the bubble frequency, breakdown of bubbling affected the heat transfer coefficient. In the smaller column, bubble growth was limited by the column walls, whereas in the large column bubbles could continue to grow so that the heat transfer coefficient profiles continued to evolve. Close to the column walls in both columns, h reached a maximum near the onset of turbulent fluidization. The heat transfer coefficients, as well as the dimensionless standard deviation of pressure fluctuations, scaled well as a function of $Fr=U/(gD_t)^{0.5}$. For $Fr \gtrsim 0.26$, both columns exhibited more homogenous flow across the bed, typical of turbulent fluidization. The heat transfer coefficient was then independent of radial position and maintained its maximum value. If the velocity is increased further so that there is massive entrainment from the bed, it is expected that the heat transfer coefficients will start to decrease.

ACKNOWLEDGEMENT

The authors thank the Natural Sciences and Engineering Research Council of Canada and the Cooperative Research Centre for Clean Power from Lignite, Australia for their financial and in-kind support. We also gratefully acknowledge Terry Joyce and Reiner Denke from CSIRO Minerals, Australia for their assistance in the experimental work.

NOTATION

D_b	Mean bubble diameter, m
D_t	Column diameter, m
d_t	Heater tube diameter, m

$Fr=U/(gD_t)^{0.5}$	Froude number, -
H	Expanded bed height, m
h	Heat transfer coefficient, W/m^{2}K
H_0	Static bed height, m
I	Current, A
Q_l	Heat losses, W
r/R	Relative radial location, -
T_b	Bed temperature, $^\circ$C
T_s	Surface temperature, $^\circ$C
U	Superficial gas velocity, m/s
U_c	U at onset of turbulent fluidization, m/s
U_{opt}	U corresponding to maximum heat transfer coefficient, m/s
V	Voltage, V
z	Distance above distributor, m
ε_0	Loose packed bed voidage, -
σ_{AP}	Standard deviation of pressure fluctuations, kPa

REFERENCES

Basu, P. & Dieh, R., 1985, "Heat transfer in turbulent fluidized beds", 23rd National Heat Transfer Conference. Heat Transfer - AIChE conference series, New York, pp. 62.

Bi, H.T. & Grace, J.R., 1995, "Effect of measurement method on the velocities used to demarcate the onset of turbulent fluidization", *Chemical Engineering Journal,* vol. 57, pp. 261-271.

Brereton C.M.H. & Grace J.R., 1992, “The transition to turbulent fluidization”, Chem Eng Res & Des, vol. 70, pp. 246-251.

Coleman, H., W. & Steele, W.G., 1998, *Experimentation and uncertainty analysis for engineers,* 2nd edn, Wiley & Sons, New York.

Ellis, N., Bi, H.T., Lim, C.J. & Grace, J.R., 2004, "Hydrodynamics of turbulent fluidized beds of different diameters", *Powder Technology,* vol. 141, pp. 124-136.

Glicksman L.R., Hyre M., Woloshun K., 1993, Simplified scaling relationships for fluidized beds. *Powder Technology, vol.* 77, pp. 177-199.

Hamidipour, M., Mostoufi, N., Sotudeh-Gharebagh, R. & Chaouki, J., 2005a, "Experimental investigation of particle contact time at the wall of gas fluidized beds", *Chemical Engineering Science,* vol. 60, pp. 4349-4357.

Hamidipour, M., Mostoufi, N., Sotudeh-Gharebagh, R. & Chaouki, J. 2005b, "Monitoring the particle-wall contact in a gas fluidized bed by RPT", *Powder Technology,* vol. 153, pp. 119-126.

Hovmand, S. & Davidson, J.F., 1971, "Pilot plant and laboratory scale fluidized reactors at high gas velocities; the relevance of slug flow" in *Fluidization*, eds. J.F. Davidson & D. Harrison, Academic Press, London, New York.

Matsen, J.M. 1996, "Scale-up of fluidized bed processes: Principle and practice", *Powder Technology,* vol. 88, pp. 237-244.

Mckain, D., Clark, N., Atkinson, C. & Turton, R., 1994, "Correlating local tube surface heat transfer with bubble presence in a fluidized bed", *Powder Technology,* vol. 79, pp. 69-79.

Mickley, H.S. & Fairbanks, D.F., 1955, "Mechanism of heat transfer to fluidized beds", *AIChE Journal,* vol. 1, pp. 374-384.

Mori, S. & Wen, C.Y., 1975, "Estimation of bubble diameter in gaseous fluidized beds", *AIChE Journal,* vol. 21, no. 1, pp. 109-115.

Mostoufi, N. & Chaouki, J., 2004, "Flow structure of the solids in gas-solid fluidized beds", *Chemical Engineering Science,* vol. 59, pp. 4217-4227.

Rhodes, M., 1996, "What is turbulent fluidization?", *Powder Technology,* vol. 88, pp. 3-14.

Staub, F.W. 1979, "Solids circulation in turbulent fluidized beds and heat transfer to immersed tube banks", Journal of Heat Transfer, vol. 101, pp. 391-396.

Sanderson, J., Rhodes, M. 2003, "Hydrodynamic similarity of solids motion and mixing in bubbling fluidized beds", *AICHE Journal,* vol. 49, no. 9, pp. 2317-2327.

Sun, G. & Chen, G. 1989, "Transition to turbulent fluidization and its prediction", *Fluidization VI*, eds. J.R. Grace, L.W. Shemilt & M.A. Bergougnou, Engineering Foundation, New York, N.Y., pp. 33-40.

Zabrodsky S.S., 1966 *Hydrodynamics and heat transfer in fluidized beds*, MIT Press, Mass., U.S.